

EFFECT OF CARBON CONTENT ON THE PHASE TRANSFORMATION CHARACTERISTICS, MICROSTRUCTURE AND PROPERTIES OF 500 MPa GRADE MICROALLOYED STEELS WITH NON-POLYGONAL FERRITE MICROSTRUCTURES

P. Suikkanen, P. Karjalainen, A. J. DeArdo

The influence of C in the range of 0.011-0.043 wt-% on the phase transformation characteristics, mechanical properties and microstructure of Fe-2.0Mn-0.25Mo-0.8Ni-0.05Nb-0.03Ti steel was investigated. In the dilatometric experiments, it was found that a reduction in the C content increased the phase transformation temperatures, decreased the hardness and promoted quasi-polygonal ferrite (QF) formation over granular bainitic ferrite (GBF) and bainitic ferrite (BF), but at the same time the sensitivity of the phase transformation temperatures and hardness to cooling rates was reduced. Mechanical testing of laboratory hot rolled plates revealed that the targeted yield strength of 500 MPa was reached even in the steel with the lowest C content (0.011wt-%). An increase in C content did not considerably increase the yield strength, although the tensile strength was more significantly increased. Impact toughness properties, in turn, were markedly deteriorated due to this C content increment. Microstructural analysis of the hot rolled plates showed that an increase in C content decreased the fraction of QF and consequently increased the fraction of GBF and BF, as well as the size and fraction of C-enriched secondary microconstituents. In addition, the size of the coarsest crystallographic packets seemed to be finer in the low C steel with QF dominated microstructure than in its higher C counterparts with higher fractions of GBF-BF, even though the average crystallographic packet size was slightly finer in these higher C steels.

Mechanical testing of the simulated CGHAZ's showed that their toughness properties are not strongly dependent on C content, although there exists a general trend for toughness to slightly weaken with increasing C content. It could be concluded that HAZ toughness properties of these types of steels are acceptable. On the basis of dilatometric experiments, mechanical testing and microstructural analysis it can be stated that a good combination of strength, toughness and weldability as well as microstructural stability can be reached in very low C steels with QF dominated microstructures. Finally, an example of this type of microstructural concept, which has been successfully

KEYWORDS: Carbon content, microalloying, austenite decomposition, microstructure, quasi-polygonal ferrite, granular bainitic ferrite, bainitic ferrite, strength, impact toughness, weldability, EBSD-IQ

INTRODUCTION

While searching for structural heavy gauge steel plates with the yield strength of 500MPa and above, high

impact toughness and good weldability, thermomechanically controlled processing of very low C microalloyed (Nb, Ti) steels with suitable combination of other alloying elements (Mn, Mo, Ni, Cu, etc.) has been established to be a potential route [1,2,3,4,5]. A desired property of these types of extremely low C steels is their relatively low sensitivity of microstructure, and thereby also mechanical properties, to the cooling rate [3,6]. Their microstructure is no longer polygonal ferrite (PF), but consists of different morphologies of non-equilibrium ferrites, such as non-polygonal ferrite and low C bainitic transformation products [1,2,7,8,9]. Quantitative characterization of these

Pasi Suikkanen, Pentti Karjalainen
University of Oulu, Finland

Anthony J. DeArdo
University of Pittsburgh, USA & University of Oulu, Finland

Paper presented at the 3rd International Conference Thermomechanical Processing of Steels, Padova, 10-12 september 2008

Code	C	Si	Mn	P	S	Cu	Ni	Cr	Mo	Nb	Ti	Al	N	Pcm
0.011C	0.011	0.19	1.98	0.003	0.004	0.22	0.82	0.03	0.26	0.052	0.034	0.03	0.005	0.16
0.024C	0.024	0.17	1.99	0.004	0.004	0.22	0.82	0.03	0.26	0.054	0.031	0.026	0.005	0.17
0.043C	0.043	0.18	1.99	0.003	0.003	0.23	0.81	0.03	0.26	0.054	0.031	0.031	0.005	0.19

$$P_{cm} = C + (Mn + Cr + Cu) / 20 + Si / 30 + Mo / 15 + V / 10 + 5B$$

▲
Tab. 1

Chemical composition of investigated steel in wt-%.

Composizione chimica in peso-% dell'acciaio esaminato.

▼
Tab. 2

The pass schedule of the hot rolling experiments.

Schema dei passaggi negli esperimenti di laminazione a caldo.

Pass no.	Temperature (°C)	Thickness (mm)	Pass reduction (%)	Total reduction (%)
		55		
1	1150	41	25	25
2	1120	30	27	45
3	880	26	13	53
4	830	22	15	60
5	810	18	18	67
6	800	15	17	73
7	790	12	20	78

kinds of mixed microstructures is difficult, which is a reason for making the comprehensive understanding of their microstructure-property combinations complicated [4,5,10].

The purpose of the present study is to investigate and understand the influence of C content in the range of 0.01-0.043 wt-% on the phase transformation characteristics and mechanical properties of Fe-2.0Mn-0.25Mo-0.8Ni-0.05Nb-0.03Ti steel with non-equilibrium ferritic microstructures. The aim is to characterize these microstructures using advanced electron optical techniques in order to understand the physical metallurgy basis of the microstructure-property combinations. Finally, an example of industrial applicability of the microstructural concept is given.

EXPERIMENTAL

The chemical compositions of investigated steels with their carbon equivalents (Pcm) are given in Tab. 1. The base composition was taken as Fe-0.2Si-2.0Mn-0.2Cu-0.8Ni-0.25Mo-0.05Nb-0.03Ti and the C content was varied at three levels: 0.011, 0.023 and 0.043wt-%. The chemical compositions presented in Tab. 1 are based on optical emission spectrometry analysis with the exception of the C contents, which were determined by using the combustion technique to achieve a better accuracy.

In order to study the phase transformation characteristics, dilatometric experiments in a Gleeble 1500 simulator were carried out. Steel pieces were soaked at 1250°C for 2 h and water quenched before machining the cylindrical specimens with a diameter of 6 mm and length of 9 mm. In the Gleeble, the specimens were reheated at 20°C/s to 1100°C and held for 2 min followed by cooling at 10°C/s to 850°C, where a single-pass compression strain of 0.6 at a rate of 0.1^s⁻¹ was applied.

After a 5 s hold, controlled continuous cooling was initiated at the rates from 0.4 to 48°C/s to room temperature.

Phase transformation start and finish temperatures were determined from the dilatometric curves and combined with the optical (OM) and field emission gun electron microscopy (FEG-SEM) microstructural analysis and hardness measurements (HV10) to construct complete continuous cooling time (CCT) diagrams. Classification of microstructures was performed according to the classification system of the Bainite Committee of ISIJ [11].

To test the mechanical properties, laboratory hot rolling trials were conducted. Slabs with the dimensions of 240 x 70 x 55 mm were normalised at 950°C for 2h and air-cooled to room temperature. The slabs were then reheated at 1250°C for 2 h after which they were hot rolled to a thickness of 12 mm using the hot rolling schedule given in Tab. 2. After the hot rolling, the plates were water-spray cooled to room temperature at the rate of about 12-15°C/s.

Tensile tests were carried out at room temperature using specimens cut parallel to the rolling direction. Two samples were tested for each plate and the average value is reported. Charpy-V testing was performed using 6 individual longitudinal specimens. The Charpy-V specimens were used to determine transition curves by testing one specimen per temperature and choosing test temperatures on the basis of previous results in a series. In this way it was possible to find out the temperatures corresponding to ductile-to-brittle transition temperature (DBTT), temperature for 27J (T27J) as well as the upper shelf energy (KV(US)) despite the limited number of specimens.

Microstructural analyses of laboratory hot rolled plates were performed using OM, FEG-SEM and EBSD measurements with the so called image quality (IQ) technique, which is a novel method for quantification of different forms of ferrite based on measuring of their lattice imperfection. The index for indication of lattice imperfection is the IQ in EBSD maps. A more detailed description of this

method can be found, for instance, in Reference [10].

In order to evaluate the weldability of steels, coarse-grained heat affected zone (CGHAZ) simulation tests were performed in a Gleeble 1500 simulator. Longitudinal specimens with dimensions of 10 x 10 x 90 mm, were extracted from the hot rolled plates. In the Gleeble, the specimens were subjected to following thermal cycle: heating at 100 °C/s to 1300 °C followed by 50 °C/s to 1350 °C, holding at 1350 °C for 1s and cooling using the Gleeble's 3D cooling program with a cooling time from 800 to 500 °C ($t_{8/5}$) of 30 s. Charpy-V and hardness tests were performed in the similar manner as described above. The standard crack tip open displacement (CTOD) specimens were tested at room temperature (23 °C) and simple mean values are reported.

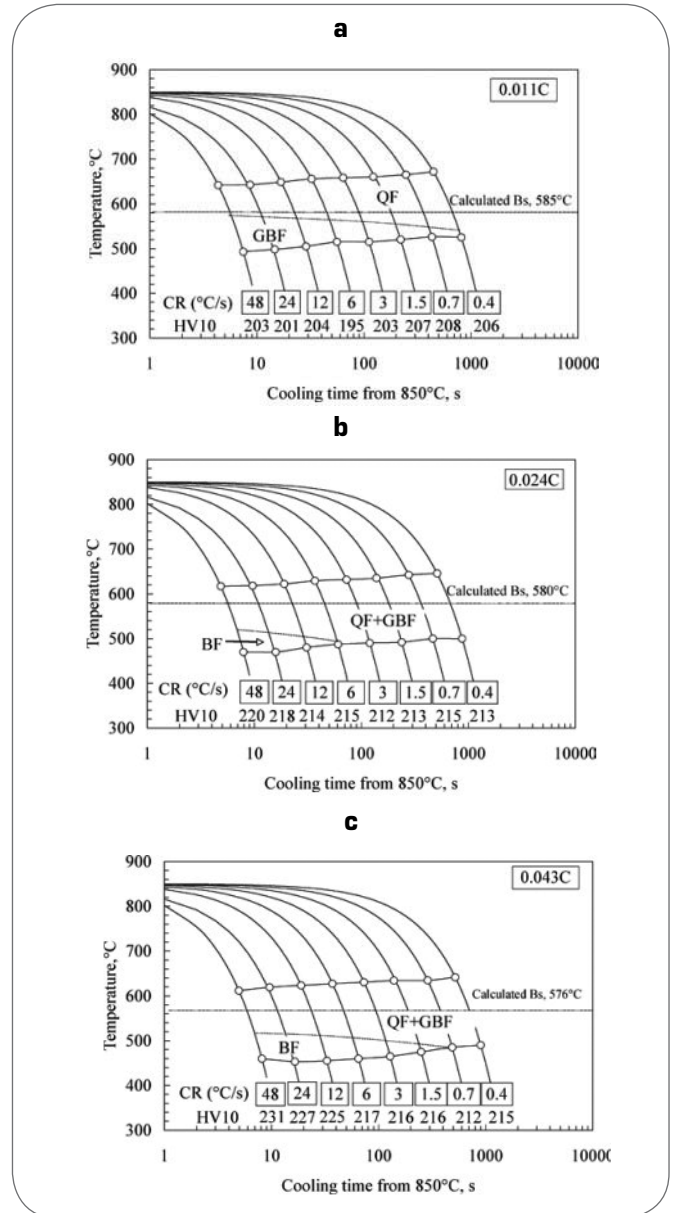
PHASE TRANSFORMATION CHARACTERISTICS AND MICROSTRUCTURES

The CCT diagrams of the investigated steels are shown in Figs. 1 a-c. A prominent feature of these steels was the low sensitivity of transformation temperatures to the cooling rates and this robustness tended to strengthen with decreasing C content, as seen by comparing Figs. 1 a-c. This observation

was further supported by the hardness values. For example, in 0.043C steel, the hardness increased by about 16 HV10 (from 215 HV10 to 231 HV10), as the cooling rate increased from 0.4 °C/s to 48 °C/s (Fig. 1 c), whereas in 0.011C steel, the hardness values were virtually unchanged over the studied cooling rate range, exhibiting values slightly above 200 HV10 (Fig. 1 a). In 0.024C steel, hardness was increased by about 10 HV10 with increasing cooling rate from 0.4 °C/s to 48 °C/s, Fig. 1 b.

As expected, for a given cooling rate, the phase transformation temperatures decreased with increasing C content. However, this decrease was not very pronounced. For instance, at the rates between 12-24 °C/s, the phase transformation start temperatures were suppressed only by 20-25 °C, when C content increased from 0.011 wt-% to 0.043 wt-%. Further, in 0.024C and 0.043C steels, the difference in phase transformation start temperatures was within 10 °C. On the other hand, the phase transformation finish temperatures seemed to be somewhat more affected by C content. At the cooling rates of 12-24 °C/s, phase transformation finish temperatures decreased by about 40-50 °C, when C content increased from minimum to maximum level. Consistent with the phase transformation temperatures, the hardness values, for a given cooling rate, were not significantly increased. For example, at the cooling rate of 12 °C/s, hardness was increased by about 20 HV10 with increasing C content from 0.011 wt-% to 0.043 wt-%.

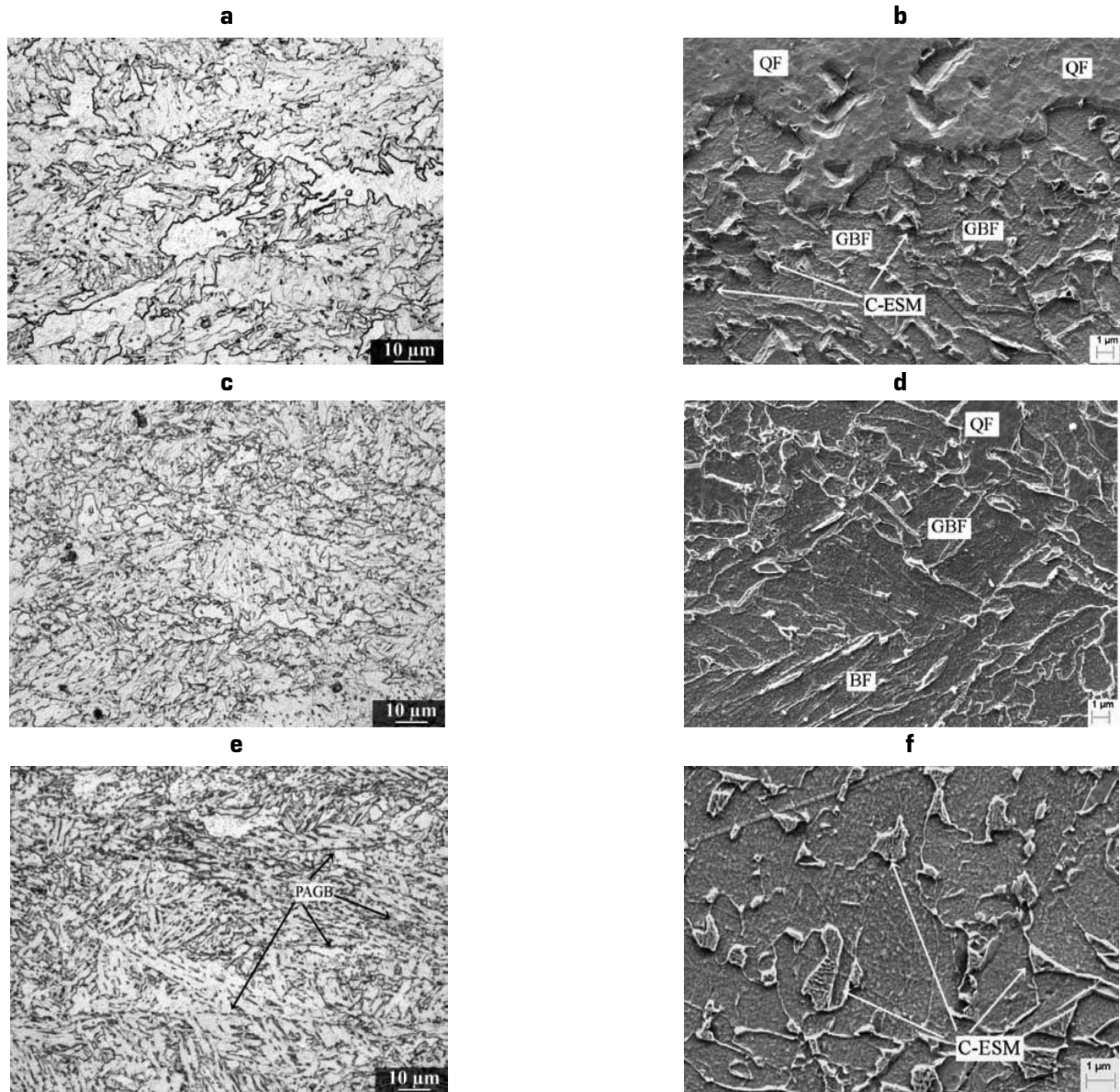
It is seen from Figs. 1 a-c, that the γ transformation in all steels initiated between 610-650 °C that is well below the estimated equilibrium temperatures, where γ transforms into PF or PF/pearlite, but still slightly higher than the estimated bainite start (Bs) temperatures. However, pronounced fractions of the γ transformations still occurred below the typical phase transformation range for low C bainite (i.e. below 550-600 °C). This would suggest that the resulting microstructures should be mixtures of non-polygonal ferrite and low C bainitic transformation products. This assumption was further confirmed by OM and SEM micrographs, as seen in Figs. 2 a-f. In the 0.011C



▲
Fig. 1

CCT-diagrams for steels (a) 0.011C, (b) 0.024C and (c) 0.043C. The Bs temperatures were estimated using an equation $B_s (°C) = 830 - 270C - 90Mn - 37Ni - 70Cr - 83Mo$ [12]. Diagrammi CCT- per acciai (a) 0.011C, (b) 0.024C e (c) 0.043C. Le temperature Bs (bainite start) sono state stimate usando l'equazione $B_s (°C) = 830 - 270C - 90Mn - 37Ni - 70Cr - 83Mo$ [12].

steel, rather coarse irregular shaped grains with highly ragged boundaries characterized the microstructures at all studied cooling rates. Between these coarse grains fine fragmented structure was observed. No clear indication of prior austenite grain boundaries (PAGB's) were detected (Fig. 2 a). Based on the OM and SEM analyses, the coarse ragged like grains were classified as QF and the fine fragmented structure as GBF according to terminology of Bainite committee of ISIJ [11]. Increasing the cooling rate slightly promoted the formation of GBF and suppressed the QF formation, but QF was still estimated to be the dominant ferrite morphology at the highest cooling rates (Fig. 1 a). No significant fractions of other fer-



▲
Fig. 2

DM and SEM micrographs of (a) and (b) 0.011C steel, (c) and (d) 0.024C steel, and (e) and (f) 0.043C steel as deformed 0.6/0.1^{s-1} at 850°C and cooled at 12°C/s to room temperature.

Micrografie DM e SEM di acciai 0.011C (a) e (b), acciai 0.024C (c) e (d), e acciai 0.043C (e) e (f), deformati 0.6/0.1^{s-1} a 850°C e raffreddati a 12°C/s fino a temperatura ambiente.

rite morphologies were found even at the highest cooling rates. In SEM micrographs, the bimodal grain structure between QF and GBF was clearly revealed, Fig. 2 b. The QF grains were much coarser than those of the GBF, which also exhibited more regular boundaries. In addition, the QF seemed to be generally free of the coarse C-enriched secondary microconstituents (C-ESM's) such as martensite-austenite (MA), but these microconstituents were mainly located inside GBF. It has been reported that all the secondary microconstituents may not necessarily be MA, but they can range from high C pearlite to conventional bainite and martensite [13], and this observation was supported by the present SEM studies. Therefore, these secondary islands are referred as C-ESM's instead of MA. In the GBF part of the microstructure, in turn, the-

se C-ESM's seemed to be frequently associated with a fine ferrite grain structure with well-etched grain boundaries, as seen in Fig. 2 b.

In the 0.024C steel, the main ferrite morphologies at low and medium cooling rates were QF and GBF, Fig. 2 b. These ferrite forms were estimated to be present at equal fractions, but the fraction of GBF for a given cooling rate was estimated to be higher than in its lower C counterpart (i.e., 0.011C steel). At the higher cooling rates (>24°C/s), the microstructure was clearly accompanied by the formation of lath like ferrite with acicular C-ESM's between the laths. This ferrite morphology was classified as BF, Fig. 2 d. Similarly to 0.011C steel, no clear indication of the PAGB's was detected, especially at the lowest cooling rates, even though some traces of

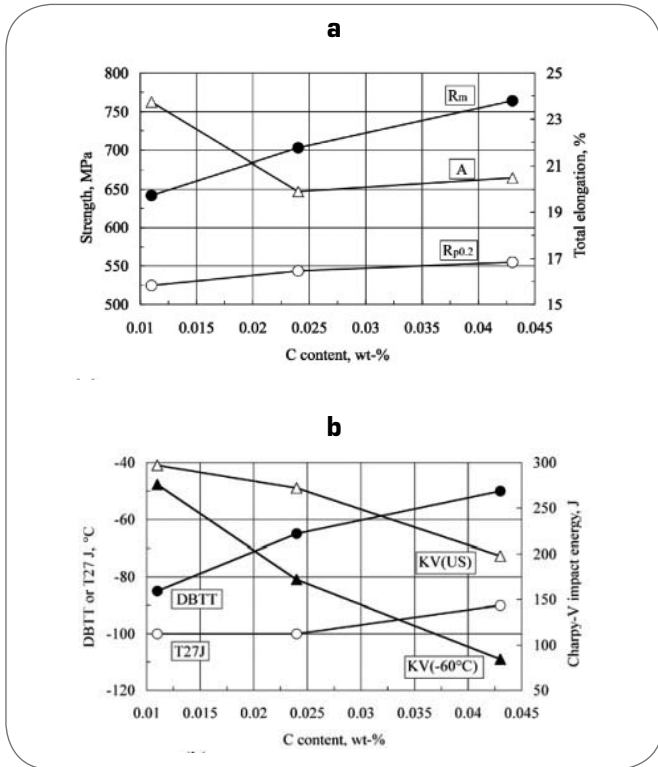


Fig. 3

Effect of C content (a) on the tensile and (b) on the impact toughness properties of laboratory hot rolled plates. Effetto del contenuto di C (a) sulle proprietà tensili e (b) sulla tenacità delle lamiere laminare a caldo in laboratorio.

these boundaries were found at the cooling rates of 24-48°C/s.

In the 0.043C steel, the fraction of QF was clearly suppressed at the lowest cooling rates, but its formation was, however, not completely eliminated even at the highest cooling rates, Fig. 1 c. The reduction of QF was consequently accompanied with the formation of increasing fractions of GBF and BF (Figs. 2 e and f) and increasing cooling rate seemed to promote especially BF formation.

Contrary to its lower C counterparts, some traces of PAGB's were occasionally observed (Fig. 2 e), which indicates that formation of QF at these sites was locally eliminated. In the SEM micrographs, the features of GBF were found to slightly differ from those of GBF observed, e.g. in 0.011C steel (Fig. 2 b). Especially, when GBF formed without any constraints of QF and transformation took place from rather coarse, weakly pancaked γ grains, the C-ESM's seemed to be distributed in a rather featureless matrix, where no distinct indications of grain boundaries were observed, Fig. 2 f.

This was contrary to the GBF in 0.011C steel, where well-discerned grain boundaries were detected in the part of the microstructure classified as GBF.

MECHANICAL PROPERTIES OF LABORATORY HOT ROLLED PLATES AND SIMULATED CGHAZ

Effect of C content on the tensile properties of the laboratory hot rolled plates is shown in Fig. 3 a. The effect of C on yield strength ($R_{p0.2}$) was not very pro-

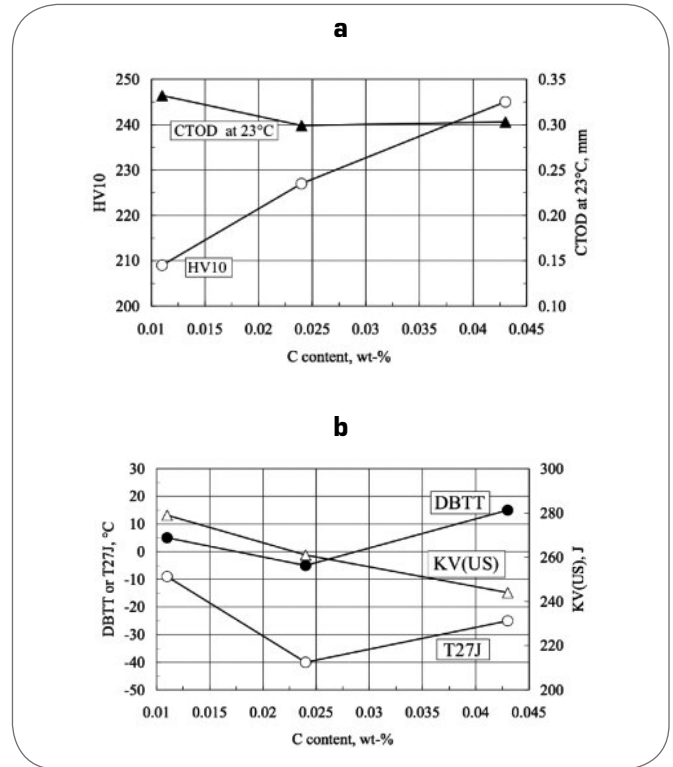


Fig. 4

Effect of C content (a) on the HV10 and CTOD and (b) on Charpy-V characteristics of the simulated CGHAZ with t8/5 of 30 s.

Effetto del contenuto di C: (a) sulle caratteristiche HV10 e CTOD e (b) sulle Charpy-V della CGHAZ (ZTA a grano grossolano) simulato con t 8/5 di 30 s.

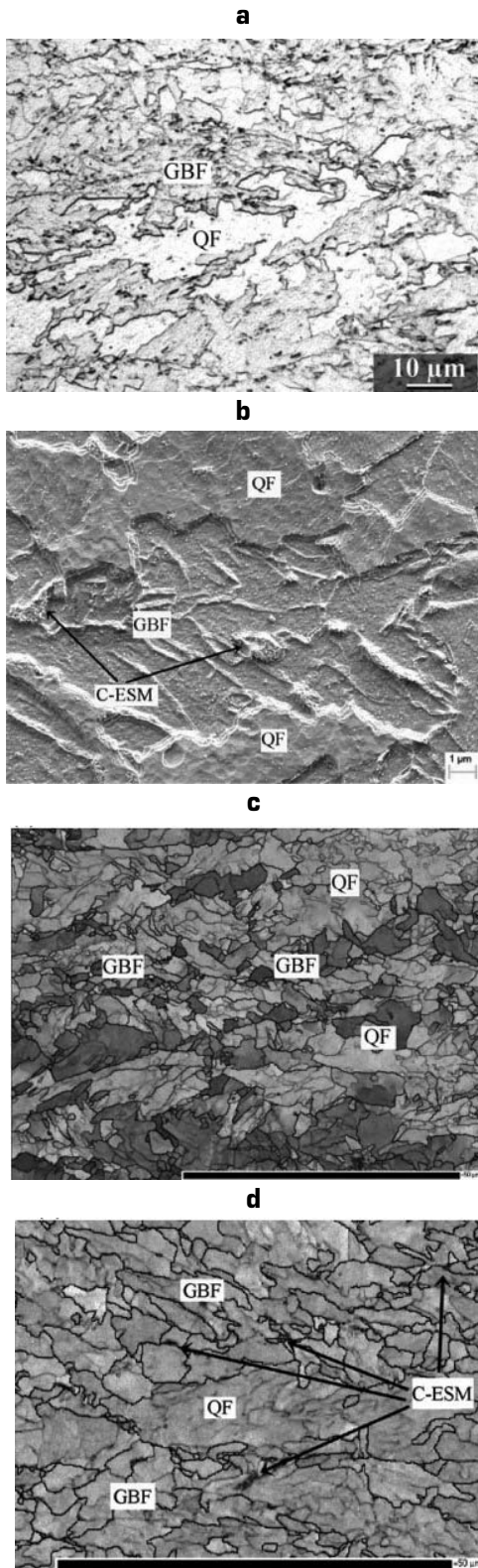
nounced; yield strength increased only by about 30 MPa, when C content increased from 0.011wt-% to 0.043wt-%. Tensile strength (R_m), in turn, was more affected and an increment of about 120MPa was obtained when C content increased from its lower limit to its upper limit studied. Total elongation (A) in 0.011C steel was above 23% and decreased to about 20% in 0.024C steel. Further increase in C content did, however, not deteriorate total elongation.

Influence of C on the Charpy-V characteristics is represented in Fig. 3 b. DBTT was below -80°C in 0.011C steel and increased rather linearly to -50°C with increasing C content. T27J, in turn, was not markedly affected by the C content, although it slightly increased with increasing C content. KV (US) decreased from 300J to slightly above 200J with increasing C. Impact energy at -60°C (KV(-60°C)) in 0.011C steel was close to its KV (US), the fracture mode being 100% ductile. KV (-60°C) decreased sharply with increasing C content, down to 80 J for 0.043C steel, where the fracture surface exhibited only about 30% of ductile features.

The mechanical properties of simulated CGHAZ's are summarized in Figs. 4 a and b. The maximum hardness of CGHAZ increased with increasing C content and it was in line with the hardness measures in the CCT diagrams at the cooling rate of 12°C/s, even though the maximum hardness of GHAZ seemed to be consistently (and expectedly) somewhat 5-15HV higher. CTOD values

Fig. 5

OM and SEM micrographs of 0.011C steel in (a) and (b), respectively. An EBSD-OIM map with LAGB's coloured as grey and HAGB's coloured as black (c). An enlargement of GBF dominated part of the microstructure as seen in EBSD-IQ image highlighting HAGB's as black (d).
 Micrografie OM e SEM dell'acciaio 0.011C, rispettivamente in (a) e (b). Una mappa EBSD-OIM (c) con bordi di grano a basso angolo (LAGB) di colore grigio e bordi di grano a alto angolo (HAGB) di colore nero. Un ingrandimento (d) della parte della microstruttura con grano ferritico bainitico (GBF) predominante, come mostrato nell'immagine EBSD-IQ che evidenzia in nero i bordi di grano a alto angolo (HAGB).



hot rolled plates. For instance, DBTT values in 0.011C and 0.024C steels were within 10°C and it was only slightly deteriorated as the C content increased to 0.043wt-%. T27] decreased by about 15°C as the C content decreased from 0.043wt-% to 0.024wt-%, but, interestingly, 0.011C steel showed the highest T27] (-10°C) among the studied steels, Fig. 4 b

MICROSTRUCTURAL CHARACTERIZATION OF LABORATORY HOT ROLLED PLATES

Consistent with the microstructures observed in the dilatometric specimens, 0.011C steel exhibited microstructure consisting of mixtures of QF and GBF, as seen in the OM and SEM micrographs in Figs. 5 a and b, respectively. Using the EBSD-IQ analysis, the volume fractions of QF and GBF were found to be 66% and 25%, respectively. The volume fraction of C-ESM's was measured as 9%.

The EBSD measurements also allowed to calculate the effective grain size, which was determined as an equivalent circle diameter (ECD) using the 15° misorientation as the angle that determines the grain. This effective grain size can be also considered as a *crystallographic packet* that is a continuous set of ferrite plates with the misorientation lower than a certain angle and it has been established to be the *microstructural unit* that controls the toughness. In general, 15° is the standard misorientation limit for high angle grain boundaries (HAGB's) and, for instance, in low C bainitic microstructures this misorientation has been found to be the critical angle for a crystallographic packet [14].

The average *crystallographic packet size* (d_{cp}) was determined as 4.1 μm. On the other hand, the grain size distribution, in SEM as well as EBSD images, revealed that the grain size distribution was not uniform at all, but consisted of rather wide distribution of finer and coarser packets.

Although the average d_{cp} was fine, 5% of the grains were coarser than ($d_{cp95\%}$) 11.5 μm and the size of the coarsest packets (d_{max}), as measured as the mean value of 10 coarsest grains in 6 EBSD maps of size of 567 x 425 μm, reached 31 μm. The size of C-ESM's, as measured from SEM images, was generally in sub-micrometer scale, the average being roughly 0.8 μm. Very coarse C-ESM's above 2 μm were only rarely detected.

As mentioned previously, QF in OM and SEM micrographs was observed to consist of coarse or massive like ragged grains that were deduced to be nucleated on the PAGB's, thereby eliminating these boundaries in the mi-

at 23°C were rather independent of C content and remained above 0.30 mm even in 0.043C steel, Fig. 4 a. KV(US) of CGHAZ decreased from 280J to 245J as the C content increased from 0.01wt% to 0.043wt-%, Fig. 4 b and exhibited rather similar dependency on the C content as KV(US) of the laboratory hot rolled plates did. DBTT and T27] values of the CGHAZ, in turn, did not show similar dependency on the C content as observed in the

Fig. 6

OM and SEM micrographs of 0.024C steel in (a) and (b), respectively. EBSD-OIM maps with LAGB's coloured as grey and HAGB's coloured as black (c). A larger EBSD-OIM map highlighting LAGB's as white (d).

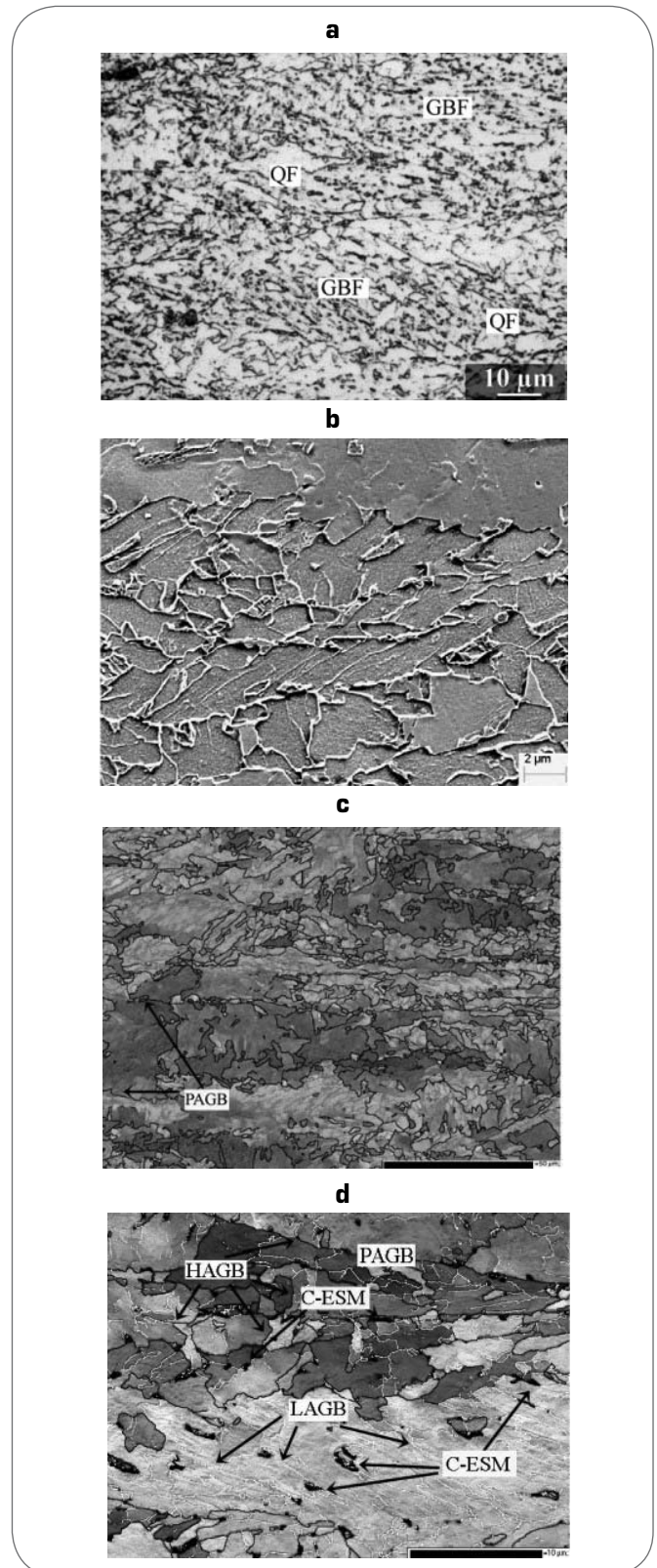
Micrografie OM e SEM dell'acciaio 0.024C rispettivamente in (a) e (b). Mappe EBSD-OIM (c) con bordi di grano a basso angolo (LAGB) di colore grigio e bordi di grano a alto angolo (HAGB) di colore nero. Un'immagine di una mappa EBSD-OIM più grande (d) che evidenzia in bianco LAGB.

crostructure, Figs. 5 a and b. In the EBSD-orientation image map (OIM) images these coarse ragged grains are well distinguishable, as seen in Fig. 5 c. Further, it was found that these QF grains contained a well-developed irregular substructure consisting of low angle grain boundaries (LAGB's) (i.e. boundaries with the misorientation lower than 15°), as also depicted in Fig. 5 c. Another typical feature of the QF grains was the lack of coarse C-ESM's, (Fig. 5 b), even though some random C-ESM's were occasionally detected inside QF. The coarser C-ESM's were mainly located in the portion of the microstructure that was classified as GBF, which, on the basis of EBSD measurements was generally found to consist of quite fine grains comprising of HAGB's (i.e. fine dcp), as seen in Figs. 5 c and d. The HAGB structure may also explain good etching response of GBF "grains" or packets in the nital seen in SEM micrographs (Fig. 5 b).

The microstructure of 0.024C steel consisted of mixtures of QF and GBF (Figs. 6 a and b). Locally some traces of lath-like ferrite with acicular C-ESM's between the laths were observed as the sign of BF formation. The fraction of QF was reduced as compared to that of 0.011C steel and this was attributed to an increase in fractions of GBF and BF as well as that of C-ESM's. However, the EBSD-IQ analysis showed that QF was still the main ferrite morphology present in the microstructure (47%), The fractions of GBF and BF was determined as 34 %, while the fraction of C-ESM's was 19%.

The mean d_{cp} and the $d_{cp95\%}$ were $3.9 \mu\text{m}$ and $10.6 \mu\text{m}$, respectively, and they were slightly finer than in 0.011C steel. However, the size of the d_{max} in 0.024C steel reached even up to $54 \mu\text{m}$. The sizes of granular shaped C-ESM's were typically ranged from $1 \mu\text{m}$ to $2 \mu\text{m}$, the mean value being $1.5 \mu\text{m}$, but some of the coarsest ones were above $3.0 \mu\text{m}$.

Steel 0.024C seemed to exhibit more microstructural heterogeneity than its lower C counterpart (i.e. 0.011C steel). In the areas, where QF was still present at significant fractions, GBF was characterized by fine fragmented structure and resembled the fine-grained GBF structure present in 0.011C steel. However, there existed locations, where the formation of QF was locally, reduced and sometimes even completely eliminated, in which case the GBF grain boundary structure seemed to be changed. The granular like C-ESM's were then located in the ferrite matrix, where the boundaries consisted mainly of LAGB's, instead being HAGB's, Figs. 6 c and d. The local fraction of QF was not the only factor influencing on the structure of GBF. The grain boundary structure of GBF developed inside different austenite grains seemed to be closely related with the thickness of pancaked grains, Fig. 6 b. Fine and well pancaked γ grains seemed to exhibit



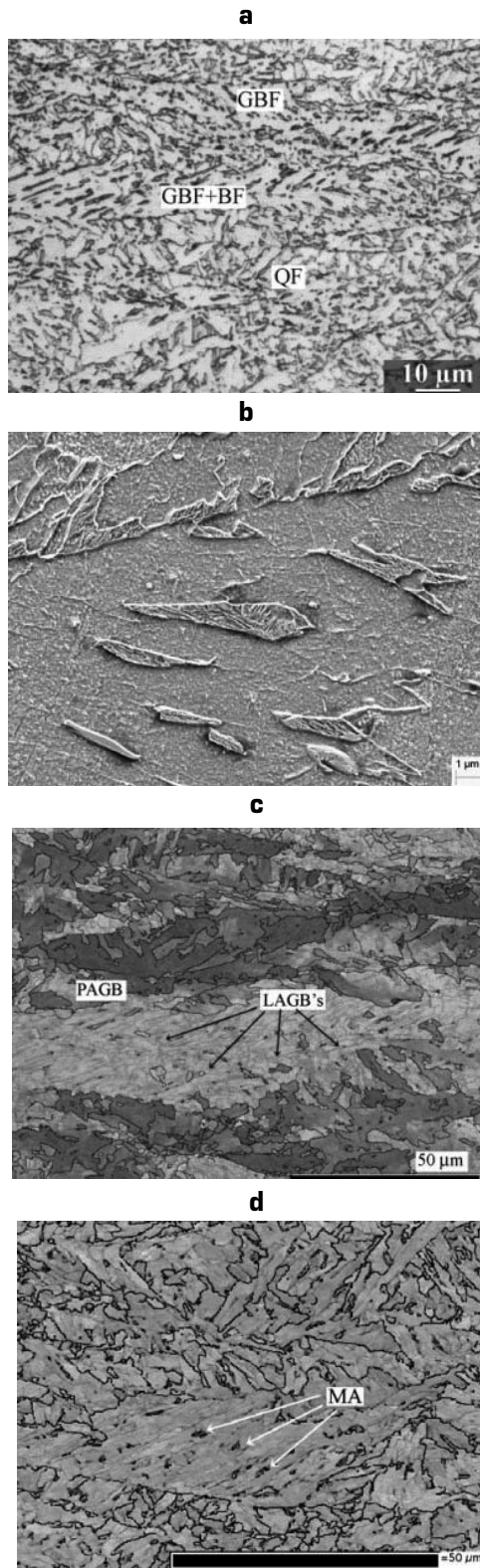
more HAGB's in the structure than the coarser and poorly pancaked ones. This relationship is probably a direct effect of different amount of accumulated strain in different γ grains.

Although the average d_{cp} and the $d_{cp95\%}$ were slightly finer in 0.024C steel than 0.011C steel, the d_{max} was coarser in 0.024C steel. This was attributed to the microstructural heterogeneity mentioned above. In the areas, where the

Fig. 7

OM and SEM micrographs of 0.043C steel in (a) and (b), respectively. EBSD-OIM maps with LAGB's coloured as grey and HAGB's coloured as black (c). EBSD-IQ image showing C-ESM's in a ferrite matrix without a close connection of HAGB's (d).

Micrografie OM e SEM dell'acciaio 0.043C, rispettivamente in (a) e (b). Mappe EBSD-OIM (c) con bordi di grano a basso angolo (LAGB) di colore grigio e bordi di grano a alto angolo (HAGB) di colore nero. Un'immagine EBSD-IQ (d) che mostra microcostituenti secondari arricchiti in C (C-ESM) in una matrice di ferrite senza una stretta relazione con HAGB.



GBF and BF. The QF was not the main ferrite morphology, the fraction being only 32%, but GBF and BF were found to dominate the microstructure with the volume fraction of 44%. Expectably, due to the highest C content, the fraction of C-ESM's was found to be the highest (24%) among the investigated steels.

The average d_{cp} and $d_{cp95\%}$ were determined as 3.4 μm and 9.5 μm , respectively, and they both were finer than the corresponding values in the lower C counterparts. However, the d_{max} size was the coarsest among the steels investigated (64 μm). The sizes of granular shaped C-ESM's were typically in the range of 1.5-2.5 μm , the average being 2.0 μm , but the size of the coarsest C-ESM's ranged from 3 μm to 5 μm .

The preservation of PAGB's was prominent in 0.043C steel. This was true in locations, where the QF formation was eliminated or its formation was significantly suppressed. Similarly to 0.024C steel, the coarsest crystallographic packets in 0.043C steel seemed to be attributed to these "QF reduced areas". Then GBF (and BF) structures tended to fill grain areas from one PAGB to another.

In these cases, the C-ESM's were located in the ferrite matrix, where the boundaries seemed to consist mainly of LAGB's, Figs. 7 c and d. Further, the preservation of PAGB's enabled the formation of the C-ESM's on these boundaries. The C-ESM's were found to be distributed on the PAGB's in a banded like structures, as seen in Fig. 7 b.

Fig. 8 is a graphical summarisation of the influence of C on the microstructural characteristics of the investigated steels. At the lowest C content the main ferrite morphology is QF with the fraction of 66%, the GBF fraction being roughly 24%. The fraction of C-ESM is then 9%. With increasing C content, the fraction of QF is reduced and this is consequently attributed to an increase in the fractions of GBF and BF. As a natural consequence of increasing C content, also the fraction of C-ESM's tends to increase. In 0.043C steel, QF is no longer the main ferrite morphology, but the microstructure is dominated by GBF and BF. The volume fraction of C-ESM's is now increased beyond 20%, Fig. 8 a. The fraction of C-ESM's was also determined by the point counting method.

The results were in line with the fraction determined by EBSD-IQ, although EBSD-IQ gave consistently somewhat higher fractions than the point counting method, as seen in Fig. 8 a.

The average d_{cp} and the $d_{cp95\%}$ sizes were slightly refined with increasing C content, which is consistent with lower phase transformation temperature in higher C

QF formation was suppressed and/or transformation took place from coarse γ grains, the GBF seemed to fill the remaining γ and then grain boundaries in this structure consisted of high fraction of LAGB's, but only very few consisted of HAGB's, leading to rather coarse crystallographic packets.

Typical microstructure of 0.043C steel is shown in Fig. 7a. The microstructure was found to consist of mixtures of QF,

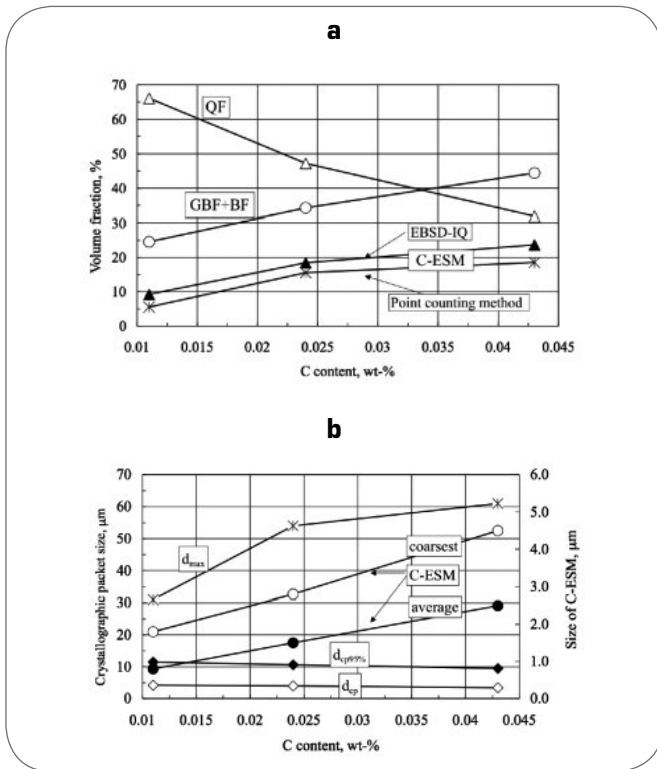


Fig. 8

Influence of C on (a) the volume fraction of various ferrite morphologies and (b) the crystallographic packet and C-ESM size.

Influenza del contenuto di C: (a) sulla frazione di volume di varie morfologie di ferrite; (b) sui pacchetti cristallini e la dimensione di C-ESM.

steels. On the other hand, d_{max} size is quite significantly increased with C content. This can be attributed to the local elimination of QF (often in coarse γ grains) and transformation of these grains into a fully GBF and BF structures characterized by a rather coarse dcp. The sizes of both the average and the coarsest C-ESM's increase with C content. In 0.043C steel the maximum size of C-ESM's can reach several micrometers, whereas in 0.011C steels both average and maximum sizes are limited.

DISCUSSION

The desired property of microstructural insensitivity to a wide range of cooling rates, as observed in CCT-diagrams in Figs. 1 a-c, can be thought to derive from the selected alloying concepts.

Especially, the utilization of strong austenite stabilizers, such as Mn and Ni, in conjunction with the low C content, explains this behaviour. Both Mn and Ni expand the temperature range for stable austenite by lowering two-phase region towards room temperature, which leads to a depression of equilibrium temperatures [15]. C, although being an austenite stabilizer, can also retard decomposition by causing a friction force between advancing γ/α interface [16] that can be assumed to increase as the cooling rate and C content increase. As the C contents in present steels are at low levels it is expected that the sensitivity of phase transformation to cooling rates are also

reduced. It is important to note that steels also contain ferrite stabilizers such as Mo, Nb and Ti, although they may raise the equilibrium temperature, they can also retard PF formation to lower cooling rates and thereby enhance steel hardenability [8]. As the reduction in C content reduces the sensitivity of phase transformation temperatures to cooling rate, also the sensitivity of hardness is diminished, since there exists a strong relationship between hardness and phase transformation start temperature in this type of steels [4,6,8].

As the initiation of phase transformation in the investigated steel was suppressed to temperatures of 610-650°C that is well below the transformation temperatures for PF, the ferrite morphology that forms first is non-polygonal QF (Figs. 2 a and b), known to form in very low C steels in the temperature range between PF and bainite [7,8,11]. QF has often been termed as massive ferrite, a transformation generally reported to occur in Fe-Mn alloys and in pure iron [7]. Massive ferrite (and therefore QF) has been suggested to form via diffusional processes and the preferential nucleation sites being the PAGB's [17], which explains the absence of these boundaries in the QF dominated microstructures. The ragged like morphology of QF has been suggested to derive from anisotropic growth, that may be a consequence of morphological instability of advancing γ/α interface [18]. At the temperature range of QF formation no long-range diffusion of substitutional atoms is expected, but interstitial atoms such as C, are still highly mobile. Therefore, it is expected that the C partition occurs from QF to residual γ , that is consequently enriched from C. This may be the reason for the small fraction of C-ESM's observed in the QF, but rather high fraction in the GBF part of the microstructure. The occasionally detected C-ESM's inside the QF might be a consequence of entrapping of C enriched γ between the growing QF interfaces [8]. The LAGB substructure observed inside the QF crystals can be thought to derive from the accommodation of strains and stresses caused by transformation at lower temperatures and/or mutual impingement of several QF crystals formed by separate nucleation events or sympathetically [19].

QF formation is often attributed to the formation of the ferrite morphology classified as GBF (Figs. 2 b and f). In low C steel (i.e. 0.011C steel) with a high fraction of QF, the GBF was frequently found to have a fine-grained structure with well-etched boundaries consisting of HAGB's (Figs. 5 b-d). On the other hand, in higher C steel (i.e. 0.043C) with reduced fractions of QF, the boundaries associated with the GBF frequently consisted of LAGB's, as in Figs. 7 c and d.

The GBF has been reported to form in the temperature range between QF and BF [7,8,9]. In the areas where QF formation was locally suppressed, the PAGB's adjacent to GBF were preserved, which indicates that it forms by a different mechanism as QF. It has been suggested that GBF is a product of Widmanstätten ferrite transformation or that GBF is essentially the similar type of transformation as BF that has just undergone significant coalescence of ferrite plates during its growth [8]. BF, in turn, has been suggested to exhibit a "genuine" bainitic type of transformation [8], similar as proposed for conventional upper bainite in higher C steels [20].

The reason for the dual character of GBF is not completely

clear, but it could be suggested that the volume change caused by a high temperature QF transformation in low C steels (such as 0.011C), causes stress and strain effects in residual γ , which influences on the way how this γ transforms into GBF. In higher C steels, the volume fraction of QF is lower and locally even completely eliminated, and thereby the stress and strain effects due to the QF formation are smaller. The GBF microstructure exhibits features that are more typical for fully GBF, i.e. granular shaped MA's in the ferrite matrix where the boundaries consist mainly of LAGB's [9]. It is interesting to note that the GBF structure in higher C steel was also fine-grained, while GBF seemed to transform from fine and highly pancaked γ grains, which may indicate that heavy deformation of austenite may change the grain boundary structure of GBF.

In CCT studies and microstructural analysis of laboratory hot rolled plates it was found that increasing C content reduced the QF fraction favouring the GBF and BF formation. Based on the CCT-diagrams and SEM and EBSD observations, the following sequence of the microstructure development can be assumed: γ starts to transform to QF at the early stage of cooling and then with increasing carbon content in the austenite the tendency of producing lath-like substructure is increased. This leads to the formation of GBF, and finally lath-like BF starts to form at the interfaces at low temperatures.

The yield strength of investigated steels with QF and GBF can be suggested to consist mainly of solid solution strengthening and transformation strengthening [1]. Solid solution strengthening consists of strengthening due to Peierls-Nabarro force and substitutional solid solution atoms (mainly by Mn). Strengthening due to interstitial atoms, such as C and N, appears to be less significant, as the transformation still takes place at the temperatures where C is highly mobile and it is very unlikely that at times and temperatures of γ/α transformation that C could be trapped inside the ferrite to such an extent that it can cause significant interstitial solid solution strengthening.

Furthermore, all steels contain strong nitride formers, such as Ti and Nb, and therefore any strengthening due to "free" N is not expected. Transformation strengthening covers the strengthening due to LAGB's, HAGB's and "free" dislocations that, in turn, can be considered to be functions of prior γ microstructure, alloy content and cooling path. Precipitation strengthening due to fine microalloy precipitates, such as NbC, may not play a significant role, if any, owing to insufficient precipitation kinetics deriving from the low phase transformation temperatures and rather high cooling rate above 10°C/s [21]. As the substitutional alloying content in the steels are identical and austenite conditioning and cooling were performed in an identical manner, the only yield strength increasing element is the C content. On the basis of CCT-diagrams (Figs. 1 a-c), C in the studied range, only slightly retards the phase transformations to lower temperatures. Thereby, it is not surprising that yield strength is only faintly increased by the C content in the laboratory hot rolled plates, Fig. 3 a, since there exist a linear relationship between decreasing phase transformation start temperature and increasing *yield strength* [1]. Effect of C-ESM's, although being present at high fractions, on the yield strength is assumed to play a minor role.

This is essentially due to their rather coarse size (typically $> 1 \mu\text{m}$) and the fact that their spacing is larger than the sizes of ferrite grains or laths.

Instead, the pronounced effect of C on *tensile strength* can be understood on the basis of C-ESM's since in a broad sense, these steels can be treated as "dual-phase" steels. It is well established in dual-phase steels, the work hardening rate increases when the volume fraction of hard martensite island is increased leading to a strong increment in tensile strength [22]. The strong increment in tensile strength with increasing C content (Fig. 3 a) can be attributed to the increasing work hardening rate with increasing volume fractions of hard C-ESM's, Fig. 8 a. Refinement of the size of MA islands, of course, leads to an increase in the work hardening rate, but in the present case, decrease in the volume fraction of C-ESM's is thought to be a dominant factor controlling the work hardening.

Total elongation in tensile tests, i.e. fully ductile fracture, is a function of nucleation, growth and coalesced of voids, formed around the hard C-ESM particles, and it has been shown that in low C bainitic steels an increase in MA volume fraction leads to a reduction in total fracture strain [16].

Further, a reduction in the size of these microconstituents is known to lead to an increase in fracture strain [23]. Therefore, it is expected that total elongation is improved with decreasing C content (as seen Fig. 3 a) as the size and the fraction of C-ESM's decrease, Figs. 8 a and b.

It is well established in low C bainitic steels [16] and even better in studies on toughness of HAZ in HSLA steels [24] that C-ESM's, such as MA's, are detrimental to impact toughness properties. In general, KV(US) decreases and DBTT increases as the size and fraction of hard C-ESM's increase.

Especially, KV(US) is lowered as the size and volume fraction of hard secondary phases are increased [25], but DBTT is also known to be deteriorated for the same reason [16,25]. Therefore, the measured reduction in KV(US) with increasing in C content (Fig. 3 b) can be attributed to the increase of size and fraction of C-ESM's, Fig. 8. Further, the increase in DBTT with increasing C content, as seen Fig. 3 b, can also be partly associated with the increase of size and fraction of the C-ESM's in the microstructure.

Good toughness of steels (especially as low DBTT) is often associated with high density of HAGB's that are usually present in the microstructure and are beneficial, because these boundaries act as obstacles for cleavage crack propagation. As mentioned previously, development of EBSD technique has enabled to use the concept of crystallographic packet as the continuous set of ferrite "grains" or "plates" with the misorientation lower than a certain angle. In low C bainitic steels crystallographic packet has been established to be the microstructural unit controlling the toughness properties. The critical misorientation is then found to be 15° [14], which is also considered as a standard misorientation for a HAGB. It also known that toughness of ferritic steels is not associated with average grain size or the finest grains, but the coarsest grains tend to control the toughness properties [26]. Similar reasoning can be also assumed to apply to crystallographic packet size. It was shown in Fig. 8 b that average d_{cp} and $d_{cp95\%}$ are slightly refined with increasing C content.

However, the d_{max} is quite markedly increased with

increasing C content and thereby with increasing fraction of GBF and BF. In many cases, these coarse crystallographic packets can be associated with the elimination of QF in some coarse, weakly pancaked γ grains, which tend to transform into fully GBF/BF structures. These structures were then characterized by a high fraction of LAGB's. Only a few of the boundaries were HAGB's, which means the coarse crystallographic packets. Therefore, it seems that the QF dominated microstructure of 0.011C steel is finer and more uniform, as seen in d_{max} size point of view, although the average d_{cp} is finer in its higher C counterparts (i.e. 0.024C and 0.043C steels).

It is reasonable to assume that increasing size and fraction of C-ESM's, as well as the increasing size of the d_{max} with increasing C content can primarily explain the deterioration of impact toughness properties. However, these may not be the only microstructural change affecting toughness that is taking place in microstructures with increasing C content. In 0.011C steel, the QF formation practically has eliminated the PAGB's and C-ESM's seemed to locate mainly inside the GBF part of microstructure, which, in turn, was frequently characterized by fine grains consisting of HAGB's (i.e. fine d_{cp}). Thereby, if the cleavage microcrack is initiated at the vicinity of C-ESM in this fine-grained GBF, its propagation is temporarily halted due to the HAGB's. For a microcrack to reach the critical length, after which the crack can propagate in an unstable manner, linking of neighbouring microcracks, is required, which in turn may require the rotation of the short microcracks in a shearing mode [27]. This, in turn, consumes energy and thereby improves toughness.

Increasing C content decreased the fraction of QF and consequently favoured the formation GBF/BF and C-ESM's. In the areas where QF ferrite formation was significantly suppressed or even completely eliminated (and transformation occurred from rather coarse γ grains), the C-ESM's were found to locate in SEM micrographs in a featureless matrix. In the EBSD maps, it was found that this featureless was due to location of C-ESM's in the ferrite matrix with substructure consisting of LAGB's, Figs. 6 c-d and 7 c-d. If the initiation of a microcrack occurs in or around of these C-ESM's in this type of structure, the LAGB's are not able to prevent the crack propagation and the crack can readily grow reaching the critical size after which the crack can propagate in an unstable manner [27]. In addition, the local preservation of PAGB's in higher C steels enabled the formation of C-ESM's on these boundaries. The C-ESM's were arranged in a banded like structures that is generally considered as a detrimental feature to impact toughness properties [28].

Although DBTT was markedly deteriorated with increasing C content, T27J was only slightly affected. The reason for this behaviour is not completely clear, but it was found that in QF dominated microstructures,

exhibiting rather low DBTT, transition from high absorbed energy to low absorbed energy occurred in rather narrow temperature range, whereas in microstructures consisting of mixtures of GF, GBF and BF, this transition occurred over a much wider temperature range [29].

Mechanical testing of simulated CGHAZ indicated that the toughness properties are not highly sensitive to C content. Although there seem to be a general trend for toughness properties to deteriorate with increasing C content, it is notable that lower C content did not always necessarily lead to improvement in toughness. This is true in the cases of DBTT and T27J. Microstructural investigations are required to gain better understanding on this behaviour. However, on the basis of mechanical test results it can be concluded that HAZ toughness properties of this type of steels are quite acceptable.

AN EXAMPLE OF AN INDUSTRIAL APPLICATION

Based on the results represented above, an industrial application of thermomechanically processed shipbuilding grade PC F500 W has been developed by Rautaruukki Oyj utilizing a very low C content approach and Si-Mn-Mo-Ni-Nb-Ti alloying. The microstructure of PC F500 W consists mainly of QF with a small fraction of GBF. The typical target values are given in Tab. 3 [30].

Mechanical property statistics of PC F500 W are shown in Figs. 9 a-d. The rather small scatter in the properties is due to microstructural robustness deriving from the chosen alloying concept and processing route. As mentioned above low C content with suitable alloying makes the microstructure and hence the mechanical properties insensitive to cooling rates.

The weldability of PC F500 W is good. As a result of the very low C content, the hardness of the HAZ always remains low. It is important to recognize that the weldability of these low C grades is best described by the parameter P_{cm} , given in Tab. 1. For PC F500 W this parameter remains below 0.22, despite the high strength level of the steel. The widely used IIW weldability parameter CEV cannot be used to estimate the preheat requirements, when the C content is as low as 0.04 wt-% or less. Weldability testing of PC F500 W has shown that 50 mm thick plates can be easily welded with the heat inputs of 0.65-3.5 kJ/mm. The required impact toughness energy of 27 J was then fulfilled at -60°C and in the cross weld tensile testing, the failure always took place in the base material. The maximum hardness measured in HAZ was 258 HV10. In controlled thermal severity (CTS) tests, welding at a heat input of 1 kJ/mm without preheating with an overmatching filler metal gave a maximum hardness of 285 HV10 in the HAZ without any signs of hydrogen cracking.

PC F500 W has been utilized in offshore and shipbuilding applications. The first deliveries were made in 2005 in a

Thickness (mm)	Rp0.2 (MPa)	Rm (MPa)	Total elongation (%)	KV(-70°C) Min. mean/ min. indiv. (J)
18-50	500	610-770	16	60/42

Tab. 3

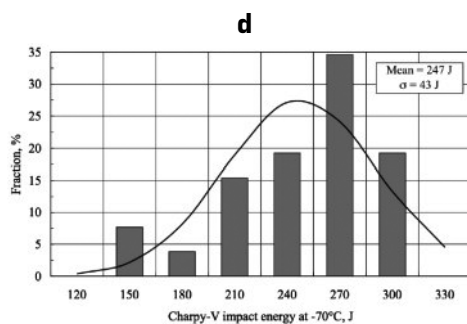
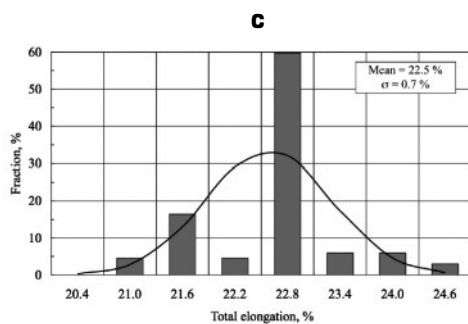
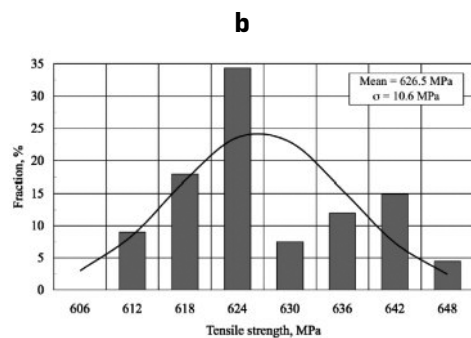
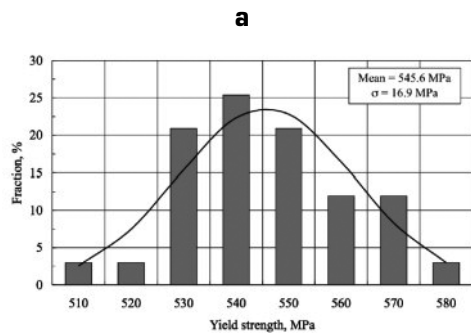
Specified minimum tensile and Charpy-V impact toughness properties for PC F500 W.

Caratteristiche minime a trazione e Charpy V specificate per PC F500 W.

Fig. 9

Mechanical properties of PC F500 W. (a) Yield strength, standard deviation (σ) = 16.9 MPa, (b) tensile strength, σ = 10.7 MPa, (c) total elongation, σ = 0.7 %, (d) Charpy-V impact toughness at -70°C with transverse specimens at quarter-thickness position, σ = 43 J.

Caratteristiche meccaniche del PC F500 W. (a) Snervamento, deviazione standard (σ) = 16.9 MPa; carico di rottura, σ = 10.7 MPa; allungamento totale, σ = 0.7 %; (d) Charpy-V a -70°C, con provini trasversali a un quarto di spessore, σ = 43 J.



Russian jack-up offshore platform project Arkticshkaya 100 [30].

SUMMARY AND CONCLUSIONS

Influence of C in the range of 0.011-0.043 wt-% on the phase transformation characteristics, mechanical properties and microstructure of 2.0Mn-0.25Mo-0.8Ni-0.05Nb-

0.03Ti steel were investigated.

In the dilatometric experiments, it was found that the phase transformation temperatures and hardness values exhibit a low sensitivity to cooling rates in the range of 0.4-48°C/s and this robustness tends even to strengthen with decreasing C content. For a given cooling rate, increasing C content, as expected, reduces both phase transformation start and finish temperatures and increases hardness, but this effect is not very pronounced. The phase transformations in these steels take place in the temperature range of about 640-480°C that is below the temperature range for PF, but partially overlaps the phase transformation temperature range of low C bainite. Microstructures consist of mixtures of different forms of non-polygonal, non-equilibrium ferrite and low C bainite, which were classified as QF, GBF and BF. It was discussed that the insensitivity of phase transformation temperatures and hardness values to cooling rates derives from low C contents and selected alloying contents (Mn, Ni, etc.). This type of alloying concepts suppresses the PF formation and favours the formation of non-polygonal ferrite and low C bainite, such as QF and GBF, over the wide cooling rate range.

Mechanical testing of laboratory hot rolled plates showed that the targeted yield strength of 500MPa is exceeded even in steel with the lowest C (i.e. 0.011C steel). However, C in the studied range, does not seem to have a pronounced effect on the yield strength, even though tensile is more pronouncedly influenced. KV(US), DBTT and KV(-60°C) are all markedly deteriorated with increasing C content. However, there is no strong effect of C on the T27J.

Mechanical testing of simulated GHAZ's showed that maximum hardness of GHAZ increased linearly with the C content. KV(US) decreases with increasing C content, but DBTT and T27J are not strongly dependent on the C content and lowering of C content does not always seem lead to an improvement in DBTT or T27J. Similarly, CTOD-values seem to be only weakly deteriorated with increasing C content. On the basis of these results, it was concluded that weldability of these steels are acceptable even with the highest C contents.

The microstructures of the laboratory hot rolled plates consist of mixtures of QF, GBF and BF. At the lowest C level (0.011wt-%), QF dominates the microstructure. With increasing C content, the fraction of QF is reduced, which consequently increases the fractions of GBF and BF. In addition, the size and fraction of C-ESM's tend to increase with increasing C content. The average d_{cp} and $d_{cp95\%}$ are slightly refined with increasing C content, and thereby

with increasing GBF and BF fractions. However, the d_{\max} seems to be refined with decreasing C content thereby with increasing fraction of QF. Hence, the crystallographic packet size is finer in lower C steel with QF dominated microstructure in the coarsest packet point of view.

It was found that a good combination of strength ($R_{p0.2} > 500\text{MPa}$) and impact toughness ($\text{DBTT} < -80^\circ\text{C}$) can be achieved in very low C steel (0.011C). The microstructure of this steel consists mainly of QF with a small fraction of GBF. The high strength of this type of microstructure is presumably derived from substitutional solid solution strengthening as well as transformation strengthening due to low γ -to- α transformation temperatures. The better impact toughness properties of low C steel with QF dominated microstructure (i.e. 0.011C steel) over its higher C counterparts (steels 0.024C and 0.043C) were concluded to be mainly a consequence of low fraction and small size of C-ESM's, as well as the refinement of the coarsest crystallographic packets. Other beneficial microstructural features in this low C steel with QF dominated microstructure were the elimination PAGB's due the formation of QF that can effectively reduce the microstructures sensitivity to prior γ structure, and the concentration of coarsest C-ESM's in the GBF part of microstructure characterized by a fine dcp. QF, in turn, was found to be virtually free of coarse C-ESM's.

Very low-C Mn-Mo-Ni-Nb-Ti steels with QF dominated microstructures have proved their capacity also in an industrial scale manufacturing. A thermomechanically processed 500MPa grade heavy gauge offshore plate developed exhibits a good combination of strength, toughness and weldability.

Due to a well-selected alloying concept and processing route, the scatter in mechanical properties is small.

REFERENCES

- 1] C.I. GARCIA, Proc. Int. Conf. Microalloying '95, Pittsburgh, PA, The ISS, Warrendale, PA (1995), p. 365.
- 2] A.J. DEARDO, Accelerated Cooling: A Physical Metallurgy Perspective. Pergamon Press, New York, (1988), p. 3.
- 3] K. FUMIMARU, H. TOSHIYUKI and A. KENITI, La Rev. Metall. 97, (2000), p. 1235.
- 4] P.P. SUIKKANEN, J.I. KÖMI and L.P. KARJALAINEN, Met. Sci. Heat Treat., 47, (2005), p. 507.
- 5] P.P. SUIKKANEN, J.I. KÖMI and L.P. KARJALAINEN, Mater. Sci. Forum, 500-501, (2005), p. 535.
- 6] T. HASE, T. HOSHINO and K. AMANO, Kawasaki Steel Tech. Rep., No. 47 (2002), 35.
- 7] T. ARAKI and K. SHIBATA, HSLA Steels '95, Beijing, China, Science and Technology Press, Beijing, China (1995), p. 13.
- 8] P. CIZEK, B.P. WYNNE, C.H.J. DAVIES, B.C. MUDLLE and P.D. HODGSON, Metall. Mat. Trans. A, 33A, (2002), p. 1331.
- 9] G. KRAUSS and S.W. Thompson, ISIJ Int., 35, (1995), p. 937.
- 10] J. WU, P.J. WRAY, C.I. GARCIA, M. HUA and A.J. DEARDO, ISIJ Int., 45, (2005), p. 254.
- 11] T. ARAKI, Atlas for Bainitic Microstructures, Iron and Steel Inst. Japan, Tokyo, (1992), p. 4.
- 12] W. STEVEN and A. J. HANSEN, J. Iron and Steel. Inst., 189 (1956), p. 349.
- 13] S. ZAJAC, Proc. of Int. Conf. on Microalloying for New Steels Processes and Application, San Sebastian, Spain (2005), Trans Tech Publication, Zurich, Switzerland, (2005), p. 387.
- 14] M. DIAZ-FUENTES, A. IZA-MENDIA and I. GUTIERREZ, Metall. Mater. Trans. A, 43A, (2003), p. 2505.
- 15] R.W.K. HONEYCOMBE, Steels – Microstructure and Properties. Edward Arnold Publishers, London (1982), p. 55.
- 16] I.A. YAKUBTSOV and J.D. BOYD, Mater. Sci. Technol. 24, (2008), p. 221.
- 17] E.A. WILSON, ISIJ Int., 34, (1994), p. 615.
- 18] R.D. TOWNSEND and J.S. KIRKALDY, Trans. ASM., 61, p. 61.
- 19] G. SPANOS and M.G. HALL, Metall. Mater. Trans. A, 27A, (1996), p. 1519.
- 20] H.K.D.H. BHADESHIA, Bainite in Steels, IOM Communications Ltd, London (2001), p. 189.
- 21] C. KLINKENBERG, K. HULKA and W. BLECK, Steel Res. Int. 75, (2004), p. 744.
- 22] C.A.N. LANZILLOTTO and F.B. PICKERING, Met. Sci., 16 (1982), p. 371.
- 23] N.K. BALLIGER, Advances in Physical Metallurgy and Applications of Steels, The Metals Society, London (1978), p. 72.
- 24] F. MATSUDA, Y. FUKADA, H. OKADA and C. Shiga, Welding in the World, 37, (1996), p. 134.
- 25] Y.M. KIM, S.Y. SHIN, H. LEE, B. HWANG, S. LEE and N.J. KIM, Metall. Mater. Trans. A, 38A, (2007), p. 1731.
- 26] C. DAVIS, Trans. Ind. Inst. Metals, 59, (2006), p. 695.
- 27] S.M. PYTEL, C.I. GARCIA and A.J. DEARDO, Proc. Int. Conf. Processing, Microstructure and Properties of Microalloyed and Other Modern High Strength Low Alloy Steels, Pittsburgh, PA, USA, (1991), The ISS, Warrendale, PA, USA (1991), p. 359.
- 28] C.L. DAVIS, Mater. Sci. Technol., 9, (1993), p. 8.
- 29] P.P. SUIKKANEN, Unpublished Research. University of Oulu, (2005).
- 30] D. PORTER, Hitsaustekniikka, 56, (2006), p. 33

ABSTRACT

EFFETTI DEL CONTENUTO DI CARBONIO SULLE CARATTERISTICHE DI TRASFORMAZIONE DI FASE, MICROSTRUTTURA E PROPRIETÀ DI ACCIAI MICROLEGATI DI GRADO 500 MPa CON MICROSTRUTTURE FERRITICHE NON POLIGONALI

Parole chiave: acciaio, trasformazioni di fase, lavorazioni plastiche a caldo

Nel presente lavoro è stata studiata l'influenza del carbonio nell'intervallo 0,011-0,043 % (in peso) sulle caratteristiche di trasformazione di fase, sulle proprietà meccaniche e sulla microstruttura dell'acciaio Fe-2.0Mn-0.25Mo-0.8Ni-0.05Nb-0.03Ti. Nelle indagini dilatometriche si è riscontrato che una riduzione del contenuto di C ha portato ad un aumento delle temperature di trasformazione di fase, ha diminuito la durezza e ha promosso la formazione di ferrite quasi poligonale (QF) rispetto alla ferrite bainitica granulare (GBF) e alla ferrite bainitica (BF), ma nel contempo ha portato a una riduzione della sensibilità alla velocità di raffreddamento sia delle temperature di trasformazione di fase e sia della durezza.

Prove meccaniche su laminati piani lavorati a caldo in laboratorio hanno evidenziato che il carico di snervamento di riferimento, pari a 500 MPa, è stato raggiunto anche nell'acciaio con contenuto di C più basso (0.011% in peso). Un aumento del contenuto di C non innalza in modo significativo il carico di snervamento, anche se ha aumentato nettamente la resistenza a trazione. Le caratteristiche di resistenza all'urto, invece, sono

risultate notevolmente peggiorate a causa di questo incremento del contenuto di C.

L'analisi microstrutturale dei laminati piani a caldo ha mostrato che un aumento nel contenuto di C ha diminuito la frazione di QF e di conseguenza ha aumentato la frazione di GBF e BF, così come le dimensioni e la frazione di microcostituenti secondari arricchiti in C. Inoltre, la dimensione dei pacchetti cristallini più ingrossati è apparsa ridotta nell'acciaio a basso C con microstruttura a prevalenza QF rispetto alla corrispondente dimensione nel caso di più alto tenore di C e maggiore presenza GBF-BF, anche se la dimensione media del pacchetto cristallino si è presentata leggermente più fine in questi acciai con più elevato tenore di C.

Le prove meccaniche sulle zone termicamente alterate a grano grossolano (coarse-grained heat affected zone - CGHAZ) simulata alla Gleeble 1500 hanno evidenziato che la loro tenacità non è fortemente dipendente dal contenuto di C, anche se esiste una tendenza generale della tenacità a diminuire leggermente con l'aumento del contenuto di C. Si potrebbe concludere che le caratteristiche di tenacità della ZTA di questi tipi di acciai sono accettabili. Sulla base delle misure dilatometriche, delle prove meccaniche e delle analisi microstrutturali si può affermare che negli acciai a tenore di C molto basso con microstruttura a prevalenza QF può essere raggiunta una buona combinazione di resistenza meccanica, saldabilità e tenacità, nonché di stabilità microstrutturale.

Infine, nel lavoro viene fornito un esempio di questo tipo di soluzione microstrutturale, che è stata utilizzata con successo in una produzione su scala industriale di un acciaio 500 MPa da off-shore.